A Microfluidic Sensing System with a Multichannel Surface Plasmon Resonance Chip: Damage-free Characterization of Cells by Pattern Recognition

Hiroka Sugai,[1] Shunsuke Tomita,[1,2*] Sayaka Ishihara,[1] Kyoko Yoshioka,[1] and Ryoji Kurita[1-3*]

[1] Biomedical Research Institute, National Institute of Advanced Industrial Science and Technology (AIST), 1-1-1 Higashi, Tsukuba, Ibaraki 305-8566, Japan.

[2] DAILAB, DBT-AIST International Center for Translational and Environmental Research (DAICENTER), National Institute of Advanced Industrial Science and Technology (AIST), Central 5-41, 1-1-1 Higashi, Tsukuba, Ibaraki 305-8565, Japan

[3] Faculty of Pure and Applied Sciences, University of Tsukuba, 1-1-1 Tennodai, Tsukuba, Ibaraki 305-8573, Japan

[*]E-mail: s.tomita@aist.go.jp; r.kurita@aist.go.jp

Abstract

The development of a versatile sensing strategy for the damage-free characterization of cultured cells is of great importance for both fundamental biological research and industrial applications. Here, we present a pattern-recognition-based cell-sensing approach using a multichannel surface plasmon resonance (SPR) chip. The chip, in which five cysteine derivatives with different structures are immobilized on Au films, is capable of generating five unique SPR sensorgrams for the cell-secreted molecules that are contained in cell culture media. An automatic statistical program was built to acquire kinetic parameters from the SPR sensorgrams and to select optimal parameters as "pattern information" for subsequent multivariate analysis. Our system rapidly (~ 10 min) provides the complex information by merely depositing a small amount of cell culture media (~ 25 μL) onto the chip, and the amount of information obtained is comparable to that furnished by a combination of conventional laborious biochemical assays. This non-invasive pattern-recognition-based cell-sensing approach could potentially be employed as a versatile tool for characterizing cells.

Introduction

With the remarkable development in stem-cell- and genome-editing technologies, cell culture systems for models to understand, diagnose, and treat diseases have received increasing attention as an alternative to conventional animal experiments.[1] Recent advances in three-dimensional culturing,[2] microfluidic technologies (so-called organ-on-a-chip),[3] and high-throughput automated cell culture systems[4] are paving the way for the use of cultured cells for industrial applications. While such technologies to control cell culture have grown rapidly, there still remain issues associated with assessing cells in culture. Representative methods for characterizing cells (e.g., types, functions, and states) include biochemical assays,[5] gene expression profiling,[6] immunofluorescence microscopy,[7] and flow cytometry.[8] However, prior to analysis, most of these require multi-step cell-damaging pre-treatments, such as trypsinization, fixing, lysis, and/or labelling; thus, rapid screening is limited and reusing cells for further culture or analysis after the assay is problematic. Although several non-invasive and label-free techniques based on Raman spectroscopy or unstained images of cell morphology have been proposed, these still require specialized equipment and knowledge in order to obtain large amounts of spectral or image data quickly and reproducibly.[9]

Holistic analysis strategies of molecules in cell culture media offer the possibility of damage-free sensing for cell characterization. Cultured cells consume and release a variety of molecules, which reflect their states and surrounding environments. These changes are regarded as a rich source of information that can help identifying various cellular characteristics.[10] For instance, metabolite profiling

of cell culture media has been proposed as a method to examine cancer cell proliferation[11] and stem cell differentiation.[12] Encouraged by the potential of cell culture media as target analytes, we have recently reported a pattern-recognition-based sensing strategy for characterizing cells based on holistic information.[13,14] These sensing methods utilize "pattern information" of optical responses coupled to differential interactions between analytes and multiple cross-reactive macromolecular probes. Because the resulting patterns include chemical properties of various components in the media, pattern-recognition using multivariate analysis can be used to accurately identify cellular properties without a highly specific molecular design.[15,16]

In previous examples of pattern-recognition-based cell sensing, including our noninvasive approaches,[13,14] response patterns are generally obtained from the use of chromogenic[13,14,17]/fluorogenic[18–21] probe materials in microplate assay platforms; however, the experimental processes, such as dispensing the probe/analyte solutions into the wells of the microplate and reading the optical signals from each well, must be repeated for the number of probes/analytes. This results in multi-step procedures, which is time consuming and prone to human error, as well as the inevitable separation of evaluation systems from cell culture systems. If the response patterns could be obtained quickly and seamlessly in one step without damaging the cells, the versatility of analytical methods based on pattern-recognition could be expanded significantly.

Inspired by the recent widespread use of microfluidic technologies in the field of cell culture,[22] we hypothesized that the application of the pattern-recognition-based sensing strategy to microfluidic

devices could adequately address the aforementioned cell-assessment challenges. In this study, we present a pattern-recognition-based sensing method using a microfluidic sensing device equipped with a multichannel sensing chip. Surface plasmon resonance (SPR) was selected as the detection mode because it is suitable for real-time, label-free,[23] and high-throughput analysis,[24,25] and the optical system can be miniaturized for implementation on hand-held instruments.[26] Our system provided an SPR response pattern that reflected the state of drug-treated cells in a single run of cell culture medium, thus allowing an easy, rapid, damage-free cell-based assay.

Results

Fabrication of multichannel chips. In SPR detection systems, the binding of analyte molecules on thin metal layers changes the refractive index in the vicinity of these thin metal layers (the so-called SPR angle shifts), which is detected as responses.[23] In this study, we used a portable SPR instrument that is capable of detecting the line profile of the SPR angle shifts. In order to obtain a SPR response pattern of cells based on just one passing of cell culture medium, we attempted to fabricate a multichannel-type chip on which various probe molecules are immobilized on separated Au films.

To construct such a sensing chip, the probe molecules should preferably be immobilized on the Au film via Au-thiol interactions and water-soluble to facilitate processing procedures such as spotting and washing. Therefore, we employed five cysteine derivatives as model cross-reactive probes to test the effectiveness of the sensing scheme [L-cysteine (Cys), *N*-acetyl-L-cysteine (Ac-Cys), L-cysteine ethyl

ester (Cys-OEt), *N*-Boc-L-cysteine (Boc-Cys), and L-penicillamine (Pen)] (Fig. 1a). As these cysteine derivatives possess distinct functional groups, analytes were expected to interact differently with the surfaces modified with each probe.

A photograph of the multichannel chip fabricated in this study is shown in Fig. 1b. The chip (18 × 18 × 4.5 mm^3) consists of main three parts (Fig. 1c): A polydimethylsiloxane (PDMS) part with two holes for the inlet and outlet of the flow path; a spacer part for the construction of a flow path with a size of 2 × 12 × 0.085 mm^3; and a substrate part with different cysteine-derivative-containing Au films in five separated compartments of a glass. In the substrate part, each compartment (width: 0.88 mm) is located at intervals of 0.54 mm (Fig. 1d). The chip was prepared by simply stacking these three parts; for details of the fabrication procedure of the chip, see Methods and Supplementary Fig. S1.

The concept of SPR sensing. A schematic illustration of pattern-recognition-based SPR sensing is summarized in Fig. 2. When an analyte solution is flown into the chip, components in the cell culture media interact non-specifically with the cysteine derivatives immobilized on the Au surfaces, thus enabling the simultaneous acquisition of SPR sensorgrams corresponding to each cysteine derivative (Fig. 2a).

Next, experimental values reflecting the feature of the analyte are extracted from the obtained SPR sensorgrams. In pattern-recognition-based sensing, the greater the number of candidate experimental values, the more preferable as the selection of appropriate experimental values is critical to accuracy. Therefore, we focused on kinetic parameters rather than intensity data after a certain time, considering

that the latter is commonly selected for pattern-recognition-based sensing.[27–30] The SPR sensorgrams contain multiple sets of information on both binding amounts and kinetics corresponding to saturated values and tangent lines, respectively; therefore, the association curves of the SPR responses (angle shifts; ΔR) are converted to 2 coefficients (a and b) according to Langmuir adsorption model: $\Delta R = a\,[1 - \exp(-bt)]$ (Fig. 2b; for details, see Methods).[31] We used an automatic analysis program developed to determine these parameters from the SPR sensorgrams.

Strictly, the nonspecific interactions between the cysteine derivatives and the medium components would not exactly be compatible with the Langmuir adsorption model because their binding stoichiometry is not 1:1. However, in pattern-recognition-based sensing, it is crucial to digitalize the trends of the SPR responses with good reproducibility for subsequent statistical analysis.

As the medium components are different depending on the cell states, each cell culture medium produces unique SPR response patterns (Fig. 2c). Subsequent multivariate analyses allow characterizing cells based on pattern-recognition.

Identification of cell types. Initially, we attempted to identify cell types from components in cell culture media to confirm the feasibility of non-invasive cell evaluation based on our SPR-based system. For that purpose, we selected three cell analytes; human-hepatocellular-carcinoma-derived cells (HepG2), human-bone-marrow-derived mesenchymal stem cells (UE7T-13), and a 1:1 mixture thereof. Analyte solutions were prepared by incubating cells in a serum-free medium (for procedural details of the cell analyte preparation, see Methods).

To obtain SPR sensorgrams, the cell culture media were introduced into the chip at a flow rate of 5.0 μL/min for 5 min after baseline equilibration. The acquisition of sensorgrams of the overall detection area was complete after 10 min using only 25 μL of the analyte solutions.

As expected, the SPR responses were observed only in the regions of the cysteine-derivative/Au/Ti thin layer on the substrate (Supplementary Fig. S2), and thus, the average sensorgrams from each region were used for the following analysis (Fig. 3a). The association curves in the SPR sensorgrams were converted to 2 coefficients as described in Fig. 2b. The thus-obtained SPR response patterns of 15 samples (3 analytes × 5 replicates) for 10 experimental values (5 probes × 2 coefficients) are summarized in Fig. 3b as a heatmap (for the raw data, see Supplementary Table S1).

In order to explore a combination of experimental values achieving high identification accuracy, a dataset for the SPR response patterns were subjected to a leave-one-out cross-validation based on Mahalanobis distances. Optimal combinations of experimental values were investigated by an exhaustive search based on ten values ($\sum_{i=2}^{10} {}_{10}C_i = 1013$ combinations) using an automatic analytical program (for details, see Methods). The exhaustive search (Supplementary Table S2) showed that 11 out of the 1013 combinations exhibit identification accuracies of 100% (15/15 samples). As shown in Supplementary Table S3, these 11 combinations consist of 5–7 experimental values from 1 or 2 coefficients of at least 3 probes. This result indicates that both the efficient digitalization of sensorgrams and the use of multiple cross-reactive probes are important to generate the differential response patterns.

Interestingly, coefficient b (primarily related to the binding rate) played a more significant role in identification than coefficient a (primarily related to the amount of saturation).

The response patterns were then subjected to linear discriminant analysis (LDA), one of the most common multivariate analyses for providing a graphical data output and insight into data clustering. LDA was carried out for a combination that required only 3 probes out of the cases achieving 100% accuracy [3 probes (Ac-Cys, Boc-Cys, and Pen) × 2 coefficients (a and b) = 6 experimental values] to visualize the complex multidimensional data as simple 2D graphics. The discriminant score plot shows the well-separated clusters corresponding to the respective analytes (Fig. 3c), indicating statistically significant differences between the SPR response patterns generated from three cell analytes, which is consistent with a cross-validation test (Supplementary Table S3). We thus conclude that (i) our SPR-based system is capable of evaluating cell-secreted components and (ii) an exhaustive search of the thus obtained datasets based on automated analysis is effective in maximizing the potential of the sensor system.

Identification of drug-treated cell states: Application to cell-based assays

After the successful identification of cell analytes without cell damage, the SPR-based system was applied to cell-based assays in drug evaluation. In the area of drug discovery, the *in-vitro* assessment of drug candidate compounds has become an essential process, where the mode of action and the effective concentration of drugs are examined from the fate and changes of cells caused by drug treatment.[32–34]

Generally, multiple cell-based assays, e.g., based on enzyme activity and staining, are performed to accurately determine the cellular responses. However, most such assays are invasive, expensive, time-consuming, and require a high level of technical skills. We thus considered that our SPR-based system can possibly overcome these limitations of conventional cell-based assays.

For a proof-of-concept study, a typical therapeutic agent for malignant tumors, tamoxifen (TAM),[35] was selected as a model drug. The delivery of drug compounds to cells induces cytotoxicity, the extent of which depends on the concentration of the drug and the exposure time.[36] Therefore, analyte media were collected after HepG2 cells were incubated in the serum-free medium at different TAM concentrations and for different exposure times (for preparation procedures of the cells, see Methods).

The cell phenotypes as a result of treatment is usually classified based on a plurality of objective indexes. Therefore, prior to pattern-recognition-based SPR sensing, the cell states after TAM treatment were classified into four groups according to the results of independent common biochemical assays (Fig. 4a); (A) alive, (B) alive/low active, (C) apoptotic, and (D) dead (for the results of the assays and the criteria of classification, see Supplementaty Note 1). In brief, the cellular states were classified according to the secretion of human serum albumin, which is an index of hepatocellular activity,[37] and the incidence of apoptosis, as well as intracellular dehydrogenase-based viability and extracellular dehydrogenase-based death of drug-treated cells. We investigated whether these cell states could be discriminated on the basis of our pattern-recognition-based SPR sensing.

The SPR responses were measured through an inflow of the analyte solutions into the chip (Supplementary Fig. S3a), then the SPR sensorgrams of 20 samples [4 analytes (group A, B, C, and D) × 5 replicates] were recorded as a training dataset (Supplementary Table S4 and Fig. S3b). Therein, no SPR signal was observed in the untreated serum-free medium with TAM (Supplementary Fig. S4). A selection of experimental values by exhaustive search revealed that 165 out of 1013 combinations show identification accuracies of 100% (20/20 samples) based on a leave-one-out cross validation (Supplementary Table S5).

In a linear discriminant score plot obtained by analyzing a combination of 8 experimental values out of the cases achieving 100% accuracy [4 probes (Cys, Ac-Cys, Cys-OEt, and Boc-Cys) × 2 coefficients (a and b)], we found that the clusters that correspond to individual groups did not overlap (Fig. 4b; for the corresponding 2D plots, see Supplementary Fig. S3c–e). Shifting from group A to D, the cluster position moved non-monotonously; the cluster initially moved in the negative direction of score (2) (A to B), then in the positive and negative direction of score (1) and score (3), respectively (B to C). Finally, it moved in the positive direction along both score (1) and score (3) (C to D). To understand these complex trends of the scores against cell states, correlation coefficients between the scores and the values of cell-based assays were calculated (Supplementary Fig. S4). Score (1) exhibits a strong correlation with the total content of protein (r = 0.99), cell death (r = 0.93), and cell viability (r = –0.99), suggesting that score (1) dominantly reflects the amount of proteins leaked from cells due to drug-induced damage. Score (2) is weakly correlated only with the albumin secretion (r = 0.51), which

thus may be associated with functional decline from group A to B. Interestingly, score (3), which was characteristic for group C, is highly correlated with apoptosis (r = –0.97). Thus, the SPR response patterns generated by just a single measurement serve as a rich source of information that can otherwise only be obtained by combining multiple biochemical assays.

Furthermore, additional 30 analytes corresponding to groups A to D (6 analytes × 5 replicates) were prepared as unknown samples for a holdout test. These unknown samples were assigned to each group generated by the training dataset shown in Fig. 4b on the basis of their Mahalanobis distances, achieving an identification accuracy of 93% (28/30 samples; Supplementary Table S4). Although one sample of group C and D were misclassed as group D and C, respectively, in a holdout test, our SPR-based system satisfyingly identified the group of the cell states in the same way as common cell-based assays. The successful identification suggests that the multichannel chip can comprehensively evaluate the mechanism of drug action on cells, including not only cell viability and death but also cellular functions such as protein production and programmed death.

Discussion

Cell culture systems as disease models strongly require long-term and real-time monitoring of cells/tissues which are subjected to stimuli such as drug treatment. Of course, conventional cell-based assays provide direct and beneficial information about particular molecules or pathways, but many of these assays exhibit several undesirable limitations, such as laborious multistep processing (e.g.,

washing, extraction, fixation, or labelling), time-consuming measurements (~ several hours), and damage to cells. Our fast and non-invasive SPR-based system has the potential to address these issues. Moreover, instead of cysteine derivatives, the use of purpose-designed recognition sites, such as self-assembled monolayers[38] and surfaces with immobilized thiol-containing peptides[39] can be expected to improve the performance and expand applications. Compared to colorimetric/fluorometric probes in previous pattern-recognition-based sensing,[40] this less restrictive probe design, in which cross-reactive probes are immobilized on Au films, can also be expected to make more hitherto unexplored chemical space accessible.

In summary, we have provided a proof-of-concept study for the development of a multichannel sensing chip for the characterization of cultured cells based on pattern-recognition of SPR responses. In this system, an optimum combination of kinetic parameters required for accurate evaluation was automatically selected by a statistical program from a plurality of SPR sensorgrams that were obtained by simultaneous measurement using a microfluidic device. Several previous studies have reported pattern-recognition-based protein sensors using SPR detection units,[27–30] but, to the best of our knowledge, our system is the first report on the SPR pattern-recognition-based sensing for cell assessment.

Our sensing approach exhibits characteristic features with significant potential benefit: (i) The design of a multichannel-type microfluidic device allows easy and rapid measurements using only a small amount of analyte solution; (ii) there is no damage to cells due to the non-invasive analysis

targeting the cell culture media; (iii) cells are characterized in multiple ways based on comprehensive information about entire components in the cell culture medium by a pattern-recognition-based sensing strategy, rather than based on analytical methods relying on specific biomarkers. The components in cell culture media are considered a rich source of information for a huge variety of biological processes.[10] Taking into account the aforementioned novel features, including the flexibility of the design of the sensing system, the reduced burden on the user on account of the automatic data analysis, and the potential connection of microfluidic cell culture devices for the purpose of on-line evaluation, our sensing device can be expected to pave the way for novel analytical approaches for cultured cells.

Author contributions

H.S., S.T., and R.K. conceived and designed the experimrnts; H.S., S.I., and K.Y. performed the experiments and analyzed the data; H.S., S.T., and R.K. wrote and edited the manuscript.

Competing interests

The authors declare no competing interests.

Acknowledgements

This research was supported by AMED under grant number JP17be0304101, by the JSPS under KAKENHI grant number JP17H04884, by a DAICENTER project grant from the DBT (Govt. of India)

to Renu Wadhwa, and a special strategic grant from AIST (Japan). A part of this work was conducted at the AIST Nano-Processing Facility, supported by "Nanotechnology Platform Program" of MEXT, Japan. We thank Dr. Mitsunori Ishihara (Research Centre for Agricultural Information Technology, National Agriculture and Food Research Organization) for help with the data analysis.

References

1. Mali, P. & Cheng, L. Concise Review: Human Cell Engineering: Cellular Reprogramming and Genome Editing. *Stem Cells* **30**, 75–81 (2012).

2. Edmondson, R., Broglie, J. J., Adcock, A. F. & Yang, L. Three-dimensional cell culture systems and their applications in drug discovery and cell-based biosensors. *Assay Drug Dev. Technol.* **12**, 207–218 (2014).

3. Ronaldson-Bouchard, K. & Vunjak-Novakovic, G. Organs-on-a-Chip: A Fast Track for Engineered Human Tissues in Drug Development. *Cell Stem Cell* **22**, 310–324 (2018).

4. Wu, Y. Y., Yong, D. & Naing, M. W. Automated Cell Expansion: Trends & Outlook of Critical Technologies. *Cell Gene Ther. Insights* **4**, 851–871 (2018).

5. Präbst, K., Engelhardt, H., Ringgeler, S. & Hübner, H. Basic Colorimetric Proliferation Assays: MTT, WST, and Resazurin. in *Cell Viability Assays: Methods and Protocols* (eds. Gilbert, D. F. & Friedrich, O.) 1–17 (Springer New York, 2017). doi:10.1007/978-1-4939-6960-9_1

6. Bhattacharya, B., Puri, S. & Puri, R. K. A review of gene expression profiling of human embryonic

stem cell lines and their differentiated progeny. *Curr. Stem Cell Res. Ther.* **4**, 98–106 (2009).

7. Atale, N., Gupta, S., Yadav, U. C. S. & Rani, V. Cell-death assessment by fluorescent and nonfluorescent cytosolic and nuclear staining techniques. *J. Microsc.* **255**, 7–19 (2014).

8. Adan, A., Alizada, G., Kiraz, Y., Baran, Y. & Nalbant, A. Flow cytometry: basic principles and applications. *Crit. Rev. Biotechnol.* **37**, 163–176 (2017).

9. Tomita, S. Noninvasive and Label-Free Characterization of Cells for Tissue Engineering Porposes. in *Biomedical Engineering Challenges: A Chemical Engineering Insight* (eds. Piemonte, V., Basile, A., Ito, T. & Marrelli, L.) 145–173 (Wiley, 2018).

10. Stastna, M. & Van Eyk, J. E. Secreted proteins as a fundamental source for biomarker discovery. *Proteomics* **12**, 722–735 (2012).

11. Jain, M. *et al.* Metabolite Profiling Identifies a Key Role for Glycine in Rapid Cancer Cell Proliferation. *Science* **336**, 1040–1044 (2012).

12. Ramm Sander, P. *et al.* Stem cell metabolic and spectroscopic profiling. *Trends Biotechnol.* **31**, 204–213 (2013).

13. Tomita, S., Sakao, M., Kurita, R., Niwa, O. & Yoshimoto, K. A polyion complex sensor array for markerless and noninvasive identification of differentiated mesenchymal stem cells from human adipose tissue. *Chem. Sci.* **6**, 5831–5836 (2015).

14. Tomita, S. *et al.* Noninvasive Fingerprinting-Based Tracking of Replicative Cellular Senescence Using a Colorimetric Polyion Complex Array. *Anal. Chem.* **90**, 6348–6352 (2018).

15. Li, Z., Askim, J. R. & Suslick, K. S. The Optoelectronic Nose: Colorimetric and Fluorometric Sensor Arrays. *Chem. Rev.* **119**, 231–292 (2019).

16. Sugai, H., Tomita, S. & Kurita, R. Pattern-recognition-based Sensor Arrays for Cell Characterization: From Materials and Data Analyses to Biomedical Applications. *Anal. Sci.* in press (2020).

17. Li, C. *et al.* An array-based approach to determine different subtype and differentiation of non-small cell lung cancer. *Theranostics* **5**, 62–70 (2015).

18. Rana, S. *et al.* A multichannel nanosensor for instantaneous readout of cancer drug mechanisms. *Nat. Nanotechnol.* **10**, 65–69 (2015).

19. Rana, S. *et al.* Ratiometric Array of Conjugated Polymers–Fluorescent Protein Provides a Robust Mammalian Cell Sensor. *J. Am. Chem. Soc.* **138**, 4522–4529 (2016).

20. Sugai, H., Tomita, S., Ishihara, S. & Kurita, R. One-Component Array Based on a Dansyl-Modified Polylysine: Generation of Differential Fluorescent Signatures for the Discrimination of Human Cells. *ACS Sensors* **4**, 827–831 (2019).

21. Tomita, S., Ishihara, S. & Kurita, R. Biomimicry Recognition of Proteins and Cells Using a Small Array of Block-Copolymers Appended with Amino Acids and Fluorophores. *ACS Appl. Mater. Interfaces* **11**, 6751–6758 (2019).

22. Choi, J., Song, H., Sung, J. H., Kim, D. & Kim, K. Microfluidic assay-based optical measurement techniques for cell analysis: A review of recent progress. *Biosens. Bioelectron.* **77**, 227–236 (2016).

23. Nguyen, H. H., Park, J., Kang, S. & Kim, M. Surface Plasmon Resonance: A Versatile Technique for

Biosensor Applications. *Sensors* **15**, 10481–10510 (2015).

24. Inoue, S. *et al.* A reliable aptamer array prepared by repeating inkjet-spotting toward on-site measurement. *Biosens. Bioelectron.* **85**, 943–949 (2016).

25. Zhang, X. *et al.* Design and performance of a portable and multichannel SPR device. *Sensors* **17**, 1435 (2017).

26. Kurita, R., Yanagisawa, H., Yoshioka, K. & Niwa, O. On-Chip Sequence-Specific Immunochemical Epigenomic Analysis Utilizing Outward-Turned Cytosine in a DNA Bulge with Handheld Surface Plasmon Resonance Equipment. *Anal. Chem.* **87**, 11581–11586 (2015).

27. Choi, S., Huang, S., Li, J. & Chae, J. Monitoring protein distributions based on patterns generated by protein adsorption behavior in a microfluidic channel. *Lab Chip* **11**, 3681–3688 (2011).

28. Uzarski, J. R. & Mello, C. M. Detection and Classification of Related Lipopolysaccharides via a Small Array of Immobilized Antimicrobial Peptides. *Anal. Chem.* **84**, 7359–7366 (2012).

29. Hou, Y. *et al.* Continuous Evolution Profiles for Electronic-Tongue-Based Analysis. *Angew. Chem. Int. Ed.* **51**, 10394–10398 (2012).

30. Wang, R., Huang, S., Li, J. & Chae, J. Probing thyroglobulin in undiluted human serum based on pattern recognition and competitive adsorption of proteins. *Appl. Phys. Lett.* **105**, 143703 (2014).

31. Wegner, G. J. *et al.* Real-Time Surface Plasmon Resonance Imaging Measurements for the Multiplexed Determination of Protein Adsorption/Desorption Kinetics and Surface Enzymatic Reactions on Peptide Microarrays. *Anal. Chem.* **76**, 5677–5684 (2004).

32. Hughes, J. P., Rees, S., Kalindjian, S. B. & Philpott, K. L. Principles of early drug discovery. *Br. J. Pharmacol.* **162**, 1239–1249 (2011).

33. Horvath, P. *et al.* Screening out irrelevant cell-based models of disease. *Nat. Rev. Drug Discov.* **15**, 751–769 (2016).

34. Moffat, J. G., Vincent, F., Lee, J. A., Eder, J. & Prunotto, M. Opportunities and challenges in phenotypic drug discovery: an industry perspective. *Nat. Rev. Drug Discov.* **16**, 531–543 (2017).

35. Shagufta & Ahmad, I. Tamoxifen a pioneering drug: An update on the therapeutic potential of tamoxifen derivatives. *Eur. J. Med. Chem.* **143**, 515–531 (2018).

36. Brandt, S., Heller, H., Schuster, K.-D. & Grote, J. Tamoxifen induces suppression of cell viability and apoptosis in the human hepatoblastoma cell line HepG2 via down-regulation of telomerase activity. *Liver Int.* **24**, 46–54 (2004).

37. Jeschke, M. G. The Hepatic Response to Thermal Injury: Is the Liver Important for Postburn Outcomes? *Mol. Med.* **15**, 337–351 (2009).

38. Minamiki, T., Ichikawa, Y. & Kurita, R. Systematic Investigation of Molecular Recognition Ability in FET-based Chemical Sensors Functionalized with a Mixed Self-Assembled Monolayer System. *ACS Appl. Mater. Interfaces* in press (2020). doi:10.1021/acsami.0c00293

39. Szymczak, L. C., Kuo, H.-Y. & Mrksich, M. Peptide Arrays: Development and Application. *Anal. Chem.* **90**, 266–282 (2018).

40. Askim, J. R., Mahmoudi, M. & Suslick, K. S. Optical sensor arrays for chemical sensing: the

optoelectronic nose. *Chem. Soc. Rev.* **42**, 8649–8682 (2013).

Methods

Fabrication of chips. The fabrication scheme of the PDMS part is summarized in Supplementary Fig. S1a. A mold (size: 20 × 20 mm^2; thickness: 4 mm) was made using a 3D printer (FlashForge Crop., Zhejiang, China). A 10:1 mixture of prepolymer and catalyst SILPOT 184 (Dow Corning Toray Co., Ltd., Tokyo, Japan) was poured in the mold and polymerized at 60 °C for 6 h. After peeling off the polymerized PDMS from the mold, two holes were drilled on a horizontal line 5 mm apart from the center of the PDMS (for the layout of the PDMS with the holes, see Supplementary Fig. S1b) using a drilling machine (Sakai Machine Tool Co., Ltd., Osaka, Japan) equipped with a drill (diameter: 0.6 mm; Saito Seisakusho Co., Ltd., Tokyo, Japan). Then, the tubes (material: fluorinated ethylene propylene; inner diameter: 0.12 mm; ALS Co., Ltd., Tokyo, Japan) were connected to the PDMS via the holes in order to deaerate *in vacuo* until immediately prior to attachment to the substrate part.

The fabrication scheme for the substraste part is summarized in Supplementary Fig. S1c. In order to generate a masking tape, a dicing tape (Denka Co., Ltd., Tokyo, Japan) was folded and the double was then cut to a size of 18 × 18 mm^2 having five rectangular holes (size: 6 × 0.88 mm at intervals of 0.54 mm; for the layout of the substrate part, see Supplementary Fig. S1d) using a cutting plotter machine CE3000-60 (Graphtec Corp., Kanagawa, Japan). After alkaline cleaning of a glass plate (material: S-BSL7; size: 18 × 18 mm^2; thickness: 0.5 mm; Iiyama Precision Glass Co., Ltd., Tokyo,

Japan), the two-layered masking tape was pasted on the glass. Then, Au/Ti films (43/5 nm) were deposited onto the glass surface using a sputtering system (CS-200; ULVAC Inc., Kanagawa, Japan). After UV/O_3 cleaning of the plate surface for 10 min using a photo surface processor (PL16-110; SEN Light Corp., Osaka, Japan), the upper masking tape was removed from the plate. Then, 1 μL of 2 mM cysteine derivatives (Cys, Ac-Cys, Cys-OEt, Boc-Cys, and Pen; Sigma-Aldrich, Co., LLC, St. Louis, MO, USA) in 10 mM sodium phosphate buffer (pH = 7.4) were spotted on each Au film and incubated for 10 min at room temperature under humid conditions. After removal of the remaining masking tape, the glass plate was washed with water to remove the excess cysteine derivatives from the Au films.

The substrate part was glued to the PDMS part via a double-sided silicone/acrylic adhesive tape (size: 18 × 18 mm^2; 2 × 12 mm^2 rectangular hole at the center; thickness: 85 μm; NTT Advanced Technology Corp., Kanagawa, Japan) as a spacer (Supplementary Fig. S1e; for the layout of the chip, see Supplementary Figs. S1f and S1g).

Preparation of the cells. Tamoxifen citrate (TAM) was purchased from Tokyo Chemical Industry Co., Ltd. (Tokyo, Japan). Dulbecco's phosphate-buffered saline (DPBS) and Dulbecco's modified eagle medium (DMEM) were purchased from Fujifilm Wako Pure Chemical Corp. (Osaka, Japan). Fetal bovine serum (FBS) was purchased from GE Healthcare UK Ltd. (Little Chalfont, Buckinghamshire, UK). Penicillin-streptomycin-neomycin antibiotic mixture and CD CHO medium were purchased from Thermo Fisher Scientific, Inc. (Waltham, MA, USA). L-Glutamine was purchased from Sigma-Aldrich, Co., LLC (St. Louis, MO, USA).

HepG2 and UE7T-13 cells were obtained from the Japanese Collection of Research Bioresources (Osaka, Japan). As cell culture media, we used a DMEM supplemented with 10% FBS, 0.5 mg/mL penicillin, 0.5 mg/mL streptomycin, and 1.0 mg/mL neomycin (DMEM++) or a serum-free CD CHO medium supplemented 8 mM L-glutamine (CDCHO+). Unless otherwise noted, cells were incubated at 37 °C in humidified air with 5% CO_2.

Cell culture media of HepG2 and/or UET7-13 cells were prepared according to our previous studies.[13,14] HepG2, UE7T-13, and 1:1 mixture of these cells (6.0×10^4 cells/well) in DMEM++ were seeded on a 24-well microplate (AGC Techno Glass Co., Ltd., Shizuoka, Japan) and incubated for 24 h. The cells were washed with DPBS (2×200 μL) and incubated with CDCHO+ (200 μL) for 48 h. The obtained cell culture media were used for the SPR experiments.

Cell culture media of TAM-treated HepG2 cells were prepared as follows. HepG2 cells (5.0×10^4 cells/well) in DMEM++ were seeded on a 96-well clear-bottom black plate (Greiner Bio-One GmbH, Frickenhausen, Germany) and incubated for 24 h. The cells were washed with DPBS (100 μL) and incubated with 0–70 μM TAM in CDCHO+ containing 0.1% DMSO (100 μL) for 0.5–12 h. The obtained cells and/or medium supernatants were used for the SPR experiments and cell-based assays.

SPR measurements. The fabricated chip was incorporated in a Smart SPR SS-1001 system (NTT Advanced Technology Corp., Kanagawa, Japan) via a matching oil (n = 1.5160; Cargille Laboratories, Inc., Cedar Grove, NJ, USA). In all SPR experiments, the solution was introduced into the chip at a flow rate of 5.0 μL/min by pulling with a syringe pump (CMA Microdialysis AB, Kista, Sweden). After baseline equilibration with

CDCHO+ for 5 min, an analyte was passed through the chip for 5 min in order to observe the association between analytes and probes. The measurements were repeated five times per analyte to generate a dataset. One chip was used for measurement of one sample solution.

Digitalization of SPR responses. According to the Langmuir adsorption model,[31] the SPR response (ΔR) corresponding to the association behavior between a analyte and a probe is described by equation 1:

$$\Delta R = \frac{\Delta R_{max}\, k_a C\, \{1 - \exp[-(k_a C + k_d)\, t\,]\}}{k_a C + k_d} \qquad (1)$$

where C is the concentration of the analyte solution and ΔR_{max} refers to the maximum SPR response obtained when all binding sites of the probes are occupied with analyte. The association rate constant and the dissociation rate constant of the interaction between the probe and analyte are k_a and k_d, respectively. Equation 1 can be simplified to:

$$\Delta R = \text{a}\,[1 - \exp(-\text{b}t)] \qquad (2)$$

where $\text{a} = (\Delta R_{max}\, k_a\, C)/(k_a\, C + k_d)$ and $\text{b} = k_a\, C + k_d$. Following equation 2, the patterns of SPR responses were described as coefficients a and b for each probe. The curve fitting was carried out using the R software (version 3.6.1).

Statistical analysis of SPR response patterns. The obtained SPR response values were statistically analyzed using the R software (version 3.6.1) in order to identify experimental values that achieve high identification accuracy. We thus constructed an analytical program that can carry out a leave-one-out cross-validation in

exhaustive combinations of experimental values. For validation, one sample was removed from a dataset, and the other samples were used to create the dataset for the validation. The removed sample was assigned to the class with the closest Mahalanobis distance to the cluster of the remaining datasets. The identification accuracy was determined on the basis of whether the sample was assigned to the correct class. To visualize the patterns, a classical linear discriminant analysis (LDA) was performed using the SYSTAT software (version 13; Systat Inc., San Jose, CA, USA).

Figures

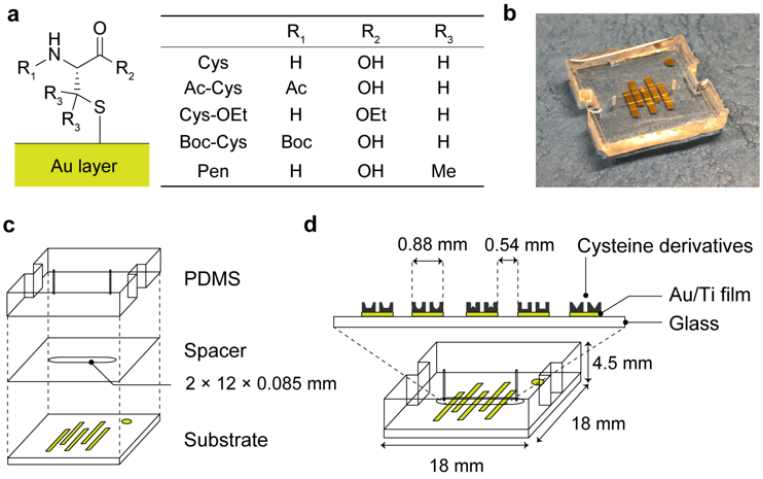

Fig. 1 Multichannel SPR chip with immobilized cysteine derivatives for pattern-recognition-based cell sensing. (a) Chemical structures of cysteine derivatives used as cross-reactive probes. (b) Photograph of the chip. (c) Perspective view showing a stacked structure of the chip. (d) Cross-sectional view of the substrate part and perspective view of the chip.

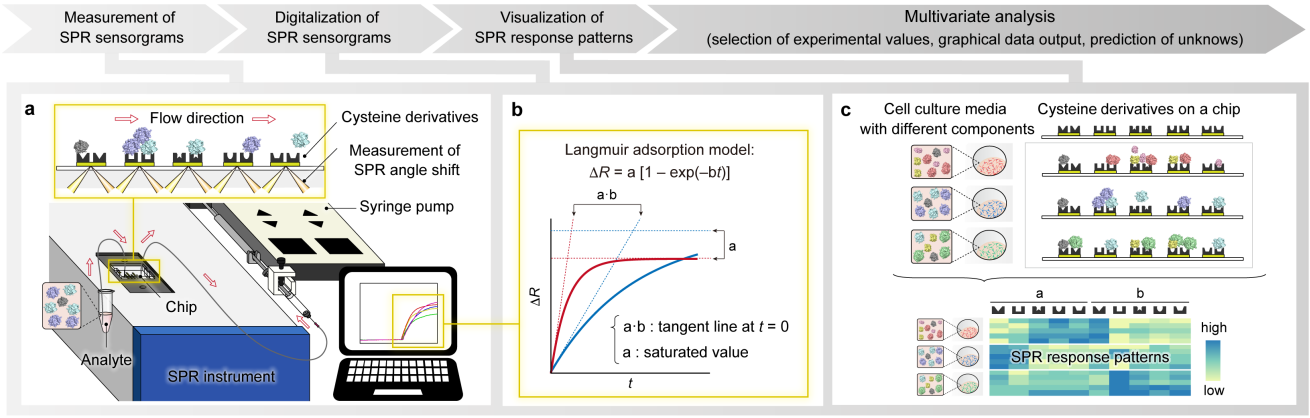

Fig. 2 Schematic illustration of pattern-recognition-based sensing of cell culture media using a multichannel SPR chip with immobilized cysteine derivatives. (a) Simultaneous acquisition of the SPR sensorgrams reflecting the interactions between cysteine derivatives on a chip and components in a cell culture medium. (b) Digitalization of the SPR sensorgrams according to Langmuir adsorption model. (c) Unique SPR response patterns resulting from cross-reactive interactions between cysteine derivatives and cell culture media with different components.

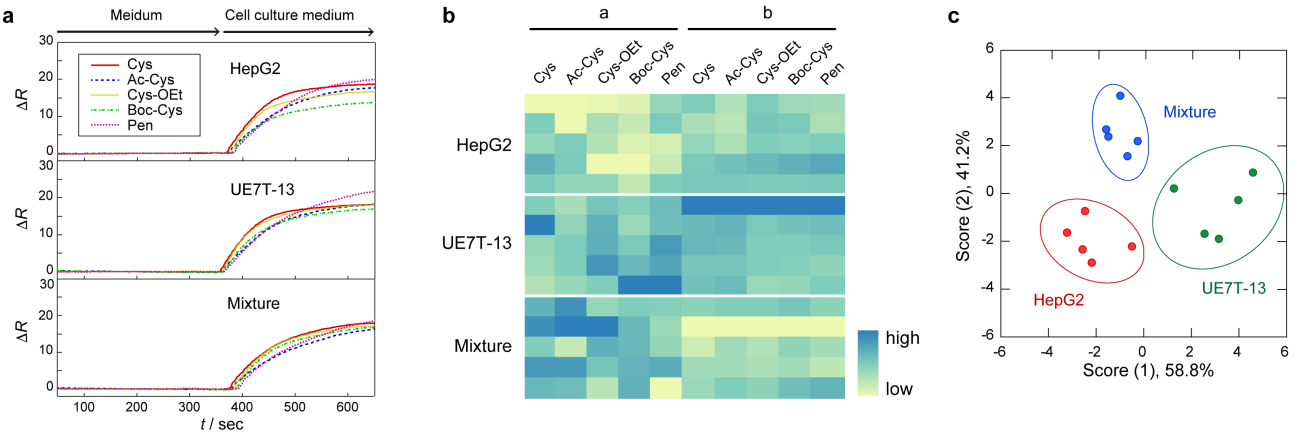

Fig. 3 Pattern-recognition-based sensing of three types of cell culture media using a multichannel SPR chip with immobilized cysteine derivatives. (a) SPR sensorgrams obtained from an inflow of cell culture

media into a chip at a flow rate 5.0 µL/min for 5 min. (b) Heat map of the SPR response patterns (n = 5). (c) Discriminant score plot obtained from the LDA of the SPR response patterns in 6 experimental values [3 probes (Ac-Cys, Boc-Cys, and Pen) × 2 coefficients (a and b)]. Ellipses represent confidence intervals ±1 SD for the individual analytes.

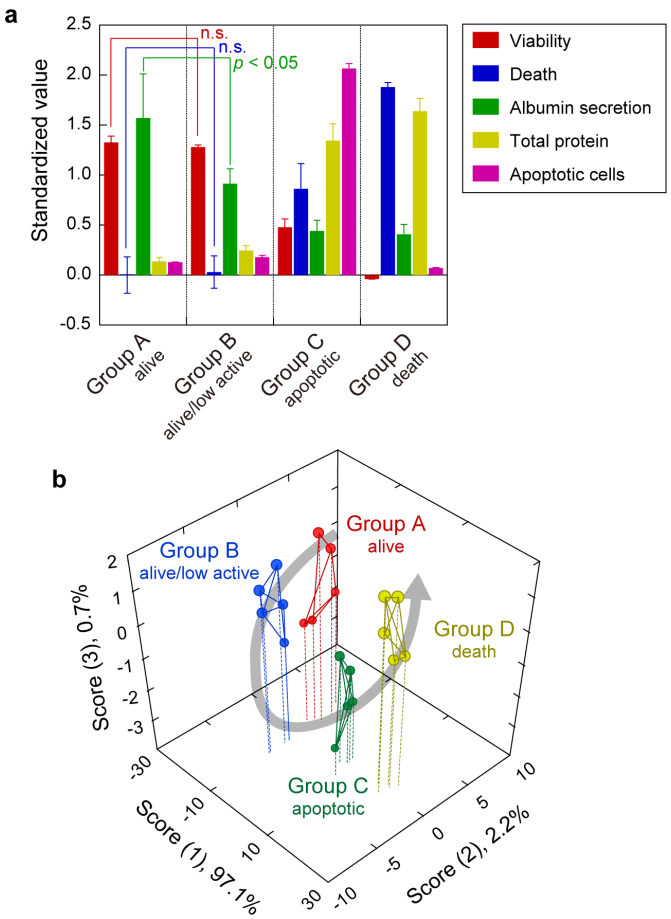

Fig. 4 Analysis of TAM-treated HepG2 cell culture media using biochemical assays or a multichannel SPR chip with immobilized cysteine derivatives. (a) Classification of cell states based on the results of independent common biochemical assays. Group A, B, C, and D correspond to the cell culture media of HepG2 cells treated without TAM for 0.5 h, with 20 µM TAM for 6 h, with 40 µM TAM for 12 h,

and with 70 μM TAM for 12 h, respectively. The vertical axis indicates the values of each biochemical assays that are standardized with root mean square (for the results of assays before standardization, see Supplementaray Figs. S6a–f). The difference between group A and B is the decrease of albumin secretion ($p < 0.05$) while there is no difference for their cell viability and death. (b) Discriminant score plot obtained from the LDA of the SPR responses in 8 experimental values [4 probes (Cys, Ac-Cys, Cys-OEt, and Boc-Cys) × 2 coefficients (a and b)].